Transcriptomic analysis of α-synuclein knockdown after T3 spinal cord injury in rats

Hong Zeng
Peking University Third Hospital Department of Rehabilitation Medicine
Bao-fu Yu
Huashan Hospital Fudan University Department of Hand Surgery
Nan Liu
Peking University Third Hospital Department of Rehabilitation Medicine
Yan-yan Yang
Peking University Third Hospital Department of Rehabilitation Medicine
Hua-yi Xing
Peking University Third Hospital Department of Rehabilitation Medicine
Xiao-xie Liu
Peking University Third Hospital Department of Rehabilitation Medicine
Mouwang Zhou (zhoumouwang@163.com)
Peking University Third Hospital https://orcid.org/0000-0003-1553-0613

Research article

Keywords: Spinal cord injury, α-Synuclein, RNA-seq, Cholinergic synapse pathway, Neurogenesis

Posted Date: August 28th, 2019

DOI: https://doi.org/10.21203/rs.2.12917/v1

Version of Record: A version of this preprint was published on November 14th, 2019. See the published version at https://doi.org/10.1186/s12864-019-6244-6.

Abstract

Abstract Background Endogenous α-synuclein (α-Syn) is involved in many pathophysiological processes in the secondary injury stage after acute spinal cord injury (SCI), and the mechanism governing these functions has not been thoroughly elucidated to date. This research aims to characterize the effect of α-Syn knockdown on transcriptional levels after SCI and to determine the mechanisms underlying α-Syn activity based on RNA-seq. Result The establishment of a rat model of lentiviral vector-mediated knockdown of α-Syn in Sprague-Dawley rats with T3 spinal cord contusion. The results of the RNA-SEQ analysis showed that there were 191 differentially expressed genes (DEGs) between the SCI group and the LV_SCI group, and 96 DEGs in the LV_SCI group compared with the sham operation group (CON group). The top 20 biological transition terms were identified by Gene ontology (GO) analysis. The Kyoto Gene and Genomic Encyclopedia (KEGG) analysis showed that the LV_SCI group significantly up-regulated the cholinergic synaptic pathway and the neuroactive ligand receptor interaction signaling pathway. Enriched chord analysis analyzes key genes. Further cluster analysis, gene and protein interaction network analysis showed that Chrm2 and Chrnb2 together observed the LV_SCI group to promote the proliferation of Chrm2 and Chrnb2 and the neurogenesis of the injury site by immunofluorescence. Further by subcellular localization, the LV_SCI group enhanced the expression of Chrnb2 at the cell membrane and cell junction. Conclusion Knockdown of α-synuclein after spinal cord injury enhance motor function and promote neurogenesis probably through enhancing cholinergic signaling pathways and neuroreceptor interactions. This study not only further clarifies the understanding of the mechanism of knockdown of α-synuclein on SCI but also helps to guide the treatment strategy for SCI.

Background

Spinal cord injury (SCI) is defined as damage to the structure and function of the spinal cord due to various causes, resulting in movement, sensation, and autonomic dysfunction below the level of injury. Primary lesions include physical trauma of white matter and gray matter and vascular system collapse followed by secondary lesions, such as demyelination, peripheral immune cell infiltration, impaired neurotransmission, and neuronal apoptosis[1]. From the destruction of tissue structure, pathophysiological changes and abnormalities of signaling pathways, the release of a large number of cytokines, proteins and metabolites may be an important factor influencing prognosis. Over the years, SCI research has been dedicated to promoting long-distance growth of CNS motor axons. The main research focus is secondary lesions, which are investigated through such methods as analysis of the regulation of the immune response[2], induction of endogenous neural stem cells[3], and neurotrophic modulators to observe changes in neurogenesis and motor function[4].

In recent years, many studies have shown that endogenous α-synuclein (α-Syn) is involved in many pathophysiological processes in the secondary injury stage after acute spinal cord injury[5]. SNCA

overexpression is a key gene that causes abnormal accumulation and aggregation of α-Syn. Intracellular aggregation of α-Syn is thought to play an important role in the pathogenesis of neurodegenerative events, including Parkinson's disease (PD) and Alzheimer's disease (AD)[6]. *In vitro* and *in vivo* experiments have reported that inhibition of α-Syn expression can reduce neuroinflammation, increase neurotrophic factor expression, inhibit apoptosis, and promote nerve regeneration[7-8]. For the production of α-Syn, aggregation or downstream effects may have strong potential for reducing the devastating complications of spinal cord injury in patients and may become the focus of future research. Nevertheless, the mechanism governing the function of α-Syn has not been determined to date.

Next-generation sequencing (NGS) has become a common technique in biology. RNA sequencing (RNA-seq) is one of the most complex applications of NGS and is a technique for sequencing and aligning RNA horizontal sequences to obtain transcriptome information. Because this method has higher accuracy than gene microarray analysis, it has higher sensitivity for detecting low-expression genes and less demand for *a priori* biological information. In addition, RNA-seq has significant advantages, such as low cost, high sensitivity, high throughput and good reproducibility. Both known and unknown transcripts can be detected by the RNA-seq method[9]. For the first time, in this study, we obtained differentially expressed genes (DEGs) by comparing the spinal cord injury group (SCI group) and the lentiviral vector-mediated knockdown SNCA (LV_SCI group) after spinal cord injury. Compared with the sham operation group (CON group), the DEGs unique to the LV_SCI group were compared for bioinformatics analysis. This study may provide new clues for studying the mechanism of SCI and provide new molecular targets for the clinical treatment of SCI.

Methods

Animals

A total of 45 SPF adult male Sprague-Dawley (SD) rats (Department of Animal Science, Peking University School of Medicine, Beijing, China) were used in this study. All the used rats were provided by the Department of Animal Science, Peking University Medical College, Beijing. All rats were housed in separate cages under a 12-hour light-dark cycle at 23 ± 1 °C and 50% relative humidity, and food and water were obtained *ad libitum*. All rats were acclimatized to the environment for at least 1 week prior to the experiment and maintained as directed by the experimental animal care and use guidelines. The study was approved by the Animal Welfare Ethics Branch of the Peking University Bioethics Committee. A completed ARRIVE guidelines checklist is included in Additional file 12: Checklist S1. Animals were randomized into three groups of 15 (n=15) each: the CON group (i.e., the sham operation group), (2) the SCI group, and (3) the SCI+LV-Snca-shRNA group (abbreviated as the LV_SCI group), and the experimental design is shown in Fig. 1A.

T3 spinal contusion model and lentiviral vector transfection knockdown of α-Syn

Lentiviral vector particles containing SNCA-shRNA (NM_019169.2) were constructed and synthesized by Shan Dong ViGene Co., Ltd. (Shandong, China). The primers for SNCA are asfollows: forward: 5'-GTGGCTGCTGCTGAGAAAAC-3', reverse: 5' -TCCATGAACGACTCCCTCCT -3'. The viral titer of LV-GFP-SNCA-shRNA was 1.0 x $10E^9$ TU/ml. All rats received prophylactic antibiotic ampicillin sodium (80 mg / kg; Harbin Pharmaceutical Group Co., Ltd., China) for three days before SCI surgery. Rats were intraperitoneally injected with 2% sodium pentobarbital (0.1 ml/kg), and the C8-T4 dorsal skin was dissected along the T2 spine *in vitro*. The muscle tissue of the back was peeled off layer by layer. The thoracic T3 segment was dissected, and the lamina of the T3 segment was removed under a surgical microscope to expose the spinal cord. In the CON group, the incision was closed layer by layer only after the spinal cord was exposed, and the SCI group was struck with the PSI-IH precision striking device (IH impactor; Precision Systems and Instrumentation, Lexington, KY, USA) after the spinal cord was exposed. The strike strength was set to 400 Kdynes, the compression time was 5 seconds, and only one hit was employed. Following SCI, 10 μl of the target gene shRNA lentiviral vector was injected *in situ* (OI) at a dose of 10 μl with a titer of 1.0 x 10E9 TU/ml using a microsyringe. The CON group and the SCI group were given the same dose of blank lentiviral vector. Two days after surgery, rats were injected subcutaneously with Ringer's sodium lactate solution (5 mL) and ampicillin sodium until the third day of injury. The rat bladder was squeezed daily 3 times after surgery until spontaneous urination was restored. All assessments and analyses were performed by researchers who were unaware of the experimental design but were experienced[33].

Behavioral Experiment

Basso, Beatlie, Bresnahan (BBB) motor function scores were used for the evaluation of hindlimb motor function[34]. The rats were placed on a circular platform with a diameter of 2 m. The walking and limb activity scores of the hind limbs were recorded. Each group was scored 1 day before surgery and on days 1, 7, 14, 21 and 28 after surgery. Rat body weight was measured daily.

Tissue Preparation

On the 28th day after surgery, all the rats were sacrificed, and a part of the spinal cord 5 mm above and below the T3 injury site was quickly placed in the cryotube for RNA-seq, and another part was verified by RT-qPCR. In addition, some tissues were used to make frozen slices. Timeline and grouping situation see additional file 11: Figure S3.

RNA extraction

Total RNA was extracted from the damaged spinal cord tissue using TRIzol® Reagent according the manufacturer's instructions (Invitrogen), and genomic DNA was removed using DNase I (TaKara). Then, RNA quality was determined by 2100 Bioanalyzer (Agilent) and quantified using the ND-2000 (NanoDrop Technologies). Only high-quality RNA samples (OD260 / 280 = 1.8 ~ 2.2, OD260 / 230 ≥ 2.0, RIN ≥ 6.5, 28S:18S ≥ 1.0, > 10 μg) were used to construct a sequencing library.

Library preparation and Illumina Hiseq xten Sequencing

An RNA-seq transcriptome library was prepared following the TruSeq^{TM} RNA sample preparation Kit from Illumina (San Diego, CA) using 5 μg of total RNA. Briefly, messenger RNA was isolated according to the polyA selection method by oligo(dT) beads and then fragmented by fragmentation buffer. Second, double-stranded cDNA was synthesized using a SuperScript double-stranded cDNA synthesis kit (Invitrogen, CA) with random hexamer primers (Illumina). Then, the synthesized cDNA was subjected to end-repair, phosphorylation and 'A' base addition according to Illumina's library construction protocol. Libraries were size-selected for cDNA target fragments of 200–300 bp on 2% Low Range Ultra Agarose followed by PCR amplified using Phusion DNA polymerase (NEB) for 15 PCR cycles. After quantification by TBS380, a paired-end RNA-seq sequencing library was sequenced with the Illumina HiSeq xten (2 × 150-bp read length).

Quality control, expression level and bioinformatics analysis

The raw paired end reads were trimmed and subjected to quality control by SeqPrep (https://github.com/jstjohn/SeqPrep) and Sickle (https://github.com/najoshi/sickle) with default parameters. To identify DEGs (differential expression genes) between two different samples, the expression level of each transcript was calculated according to the number of reads from a transcript per million reads (TPM, **Transcripts Per Million reads**) method. RSEM (http://deweylab.biostat.wisc.Edu/rsem/)[35] was used to quantify gene abundances. R statistical package software EdgeR (Empirical analysis of Digital Gene Expression in R, http://www.bioconductor.org/packages/2.12/bioc/html/edgeR.html)[36] was utilized for differential expression analysis. The raw counts were statistically analyzed using the DESeq2 software based on the negative binomial distribution. Based on certain screening conditions, genes/transcripts with differences in expression between the groups were obtained. Parameters: $p < 0.05$&$|\log2FC| >= 1$. In addition, functional-enrichment analysis including GO and KEGG was performed to identify which DEGs were significantly enriched in GO terms and metabolic pathways at Bonferroni-corrected P-value ≤ 0.05 compared with the whole-transcriptome background. GO functional enrichment and KEGG pathway analysis were carried out by Goatools (https://github.com/tanghaibao/Goatools) and KOBAS (http://kobas.cbi.pku.edu.cn/home.do)[37].

Real-time Quantitative PCR (RT-qPCR) verification

Real-time Quantitative PCR, total RNA was first extracted from spinal cord injury tissue of TRIzol (Invitrogen, Thermo Fisher Scientific Inc., USA) according to the manufacturer's protocol. The ratio of absorbance of A260 / 280 and A260 / 230 was then determined using an ultraviolet-visible spectrophotometer (Nanodrop 2000, Thermo Fisher Scientific, Waltham, MA, USA) to determine the purity and concentration of total RNA for each sample. Total RNA (2 μg/sample) was reacted with a fastking cDNA first strand synthesis kit (Tiangen, Beijing, China) to synthesize cDNA, and then real-time reaction was carried out using SYBR Green PCR Master Mix (Tiangen, Beijing, China). The expression level of glyceraldehyde 3-phosphate dehydrogenase (GAPDH) was used as an internal control. Three replicate wells were set up for all reaction samples and repeated three times. All primers used in this experiment were supplied by Sangon Biotech (Shanghai) Co., Ltd. (Additional file 10: Table S8 listed the primer sequences). Amplification was performed by QuantStudio Design and Analysis software (Applied Biosystems), and the melting curve analysis confirmed primer specificity. Finally, the cycle threshold (CT) fluorescence value was determined. The data were analyzed by a -ΔΔCT method by researchers blinded to the grouping of each animal.

Bromodeoxyuridine (BrdU) Administration

To label proliferating cells after spinal cord injury, rats were injected intraperitoneally (100 mg / kg) with the thymidine analogue bromodeoxyuridine (BrdU; 10 mg / mL in sterile saline; Sigma-Aldrich, 7 days prior to sampling) St. Louis, MO, USA). Each group of rats was given a specific BrdU pulse protocol[38].

Immunofluorescence

Frozen sections were thawed for 30 min at room temperature and washed three times in 0.1 mmol / L PBS (PBS-TX) containing 0.1% Triton X-100 (Sigma-Aldrich, St. Louis, MO, USA) (10 min each) and preincubated for 15 min at 37 °C in permeabilization blocking buffer (0.1 mmol / L PBS, pH 7.3, 0.5% Triton). The sections were blocked with 10% (v/v) goat serum (Boster Biological Technology, Ltd., Wuhan, China) for another 30 min. The sections were then incubated overnight with the primary antibody at 4 °C. After washing with PBS-TX for the next day (3 times, 10 min each), the second antibody was incubated for 1 h at room temperature and then washed with PBS-TX. The nuclei were stained with 4,6-diamidino-2-phenylindole (DAPI, 1 μg/mL; Sigma-Aldrich) for 5 min, washed with PBS-TX and sealed with an anti-fluorescence quencher. Images were captured under confocal fluorescence microscopy and a Leica DM4 B fluorescence microscope (Leica Microsystems Inc., Wetzlar, Germany) by Leica TCS SP8 (Leica Microsystems Inc., Wetzlar, Germany). Negative controls were performed with the corresponding isotype serum instead of the primary antibody. Dilution was performed using the following antibodies and

antibody dilutions: primary antibodies included mouse anti-DCX (1:100; Abcam, Cambridge, MA), rabbit anti-Chrm2 (1:100; Abcam, Cambridge, MA), mouse anti-BrdU (1:100; Abcam, Cambridge, MA), and rabbit anti-Chrnb2 (1:400; Abcam, Cambridge, MA). Fluorescent secondary antibodies included Alexa Fluor 647-conjugated AffiniPure goat anti-rabbit IgG (H + L) (1:800; Jackson ImmunoResearch Laboratories, West Grove, PA) and Cy3-conjugated goat anti-mouse secondary antibody (1:200; Boster Biological Technology, Ltd., Wuhan, China).

Statistical Analysis

Data are expressed as the mean ± S.D. Statistical analysis was assessed by GraphPad Prism 7.0 (GraphPad Software Inc., San Diego, CA). Comparisons between the two groups were performed using Student's t-test or the Mann-Whitney test as appropriate. One-way and two-way ANOVA and multiple comparisons of Tukey were used between groups. The BBB motor function score was analyzed by two-way repeated measurements of analysis of variance (ANOVA) followed by Holm-Sidak multiple comparison test. A P-value < 0.05 was considered statistically significant. * indicates $p < 0.05$, ** indicates $p < 0.01$, *** indicates $p < 0.001$, and **** indicates $p < 0.0001$.

Results

Experimental procedure and animal recovery

The entire experimental procedure is shown in Fig.1A. We examined the BBB exercise score throughout the experiment. The changes in rat body weight and BBB exercise score over time are shown in Fig.1B-C. Body weight was higher in the LV_SCI group than in the SCI group on day 28, and the BBB exercise score was higher in the LV_SCI group than in the SCI group on days 21 and 28, and the scores in the two groups were significantly lower than those in the CON group. It was shown that administration of LV-SNCA-shRNA can improve the functional recovery of BBB in rodents after severe T3 contusion.

Differentially expressed mRNA

To further understand the role and mechanism of knockdown of α-Syn on SCI, three sets of biological replicates were established in each group for RNA-seq. A summary of sequence assembly after sequencing of Illumina is presented in Additional file 1: Table S1. The Q30 basic mass fraction of the sample exceeded 90.06%, meeting the requirements of subsequent analysis. The utilization of the mapping between the transcriptome and the reference genome results in clean readings for further analysis (Additional file 2: Table S2). In the RNA-seq results, 32883 genes were detected, and Venn analysis between samples showed the amount of expressed genes in each group (Fig.2A). The

expression level of the total transcriptome shown by the correlation heat map was expressed by DEGs. Because the LV_SCI1 sample was poor correlation, this sample was removed from the analysis[10], and the CON group, the SCI group and the LV_SCI group were clearly distinguished (Fig.2B). In Fig. 2C, the SCI and LV_SCI group differential gene volcano maps showed that 191 genes were differentially expressed between the two groups, of which 89 genes were upregulated and 102 genes were downregulated. The upregulated and downregulated genes are listed in **A**dditional file 3: Table S3 and Additional file 4: Table S4. Figure 2D shows the volcano map of the differential gene between SCI and CON. The results showed that 1680 genes were differentially expressed between the two groups, of which 818 genes were upregulated and 862 genes were downregulated.

GO function enrichment analysis

To further explore the effect of knocking down α-Syn on the regulation of SCI, the GO database was used to analyze the function set information between the groups, and the significance of the function set to the differentially expressed genes was calculated. Fig.3A shows the enrichment results of the GO enrichment display TOP20 of the 191 DEGs in the SCI group and the LV_SCI group based on the DEG-based biological process (BP) category (Additional file 5: Table S5). Among these DEGs, the "extracellular matrix", "ion channel activity", "passive transmembrane transporter activity" and other regulatory enrichment rates are the highest. The Venn analysis of Fig.3B demonstrates the regulation of DEGs specific to SCI relative to spinal cord injury and normal spinal knockdown a-Syn, while GO enrichment of its 96 DEGs (Fig.3C). The exclusive of GO terms of in LV_SCI group compared to the other two groups are listed in Additional file 6: Table S6**.** The "extracellular matrix", "positive regulation of mesenchymal cell proliferation involved in ureter development" and "neurotransmitter transport" are highly enriched. Taken together, the results of this analysis indicate that knocking down α-Syn primarily affects cell transport-related biological processes.

KEGG pathway analysis

The KEGG pathway enrichment assay further determines the signaling pathways involved in DEGs. The bubble map of the differential gene provides a graphical representation of the top 20 most enriched pathways of DEGs (Fig.4A). Enriched KEGG pathways from the differentially expressed genes are listed in Additional file 7: Table S7**.**Among the many enriched signaling pathways, the cholinergic synapse pathway and neuroactive ligand-receptor interaction were the most significant. Further enrichment chord analysis (Fig.4B) showed that significantly upregulated Chrm2 and Chrnb2 were involved in both conduction pathways. At the same time, further clustering analysis was performed on the two differential signaling pathways (Fig.4C-D). The differential genes involved in the cholinergic synapse pathway are Kcnj12, Chrnb2, Kcnj14, Slc5a7, Chat, Chrm2, and Slc18a3. Among the neuroactive ligand-receptor interactions are Gabrb2, Grik3, Htr2a, Glra1, Chrnb2, Adra1d, Chrm2, and Grm3. All 13 differentially

expressed genes are listed in S3 for reference. Figures 4E-F show KO (KEGG Ontology) plots for both, and all products with a colored background in the figure belong to the sequencing gene/transcript KEGG background annotation results. KEGG mapping of cholinergic signaling pathways and neuroreceptor interactions pathways showed in Additional file 8: Figure S1 and Additional file 9: Figure S2.

Gene and protein interaction network analysis

Chrm2 and Chrnb2 were used as genes of interest to analyze the correlation between gene expression, and the correlation coefficient between gene and gene was obtained using the Spearman correlation algorithm and then mapped into a visualization network (Fig.5A). The internode connection represents that there is a correlation between gene expression, and the larger the node is, the stronger the correlation is between the gene and the expression of other genes. The differential genes with high correlation with Chrm2 and Chrnb2 are Ccl4, Adra1d, Fam135b, Atp8a2, RGD1309108, Chat, Cdh7, Slc5a7, Chodl, Lingo4, and Pcdh20. According to the protein interaction relationship contained in the STRING database, the SCI group and the LV_SCI group's DEGs are mapped to the interaction relationship for network construction, and the key nodes in the interaction network are obtained according to the intergene connectivity and other indicators (Fig.5B). The results showed that Chrnb2 interacted directly with Chrm2, and the relative expression of the Chrnb2 gene has a higher degree of centrality (DC), indicating that this gene is more strongly associated with other proteins. This gene can be speculated to play a more important role in the LV_SCI group.

RT-qPCR verification of RNA-seq

Fig.6A shows TPM changes of 13 DEGs in RNA-seq. To further validate the transcriptome sequencing results of DEGs, differentially expressed mRNA from 13 Cholinergic synapse pathway and Neuroactive ligand-receptor interaction pathways was verified by RT-qPCR (Fig.6A). Gapdh is used as an internal reference. (Fig.6B). Correlation analysis was performed based on the Log2FoldChange value of DEGs, and the correlation coefficient was 0.6353 (P=0.0196) (Fig.6C).

Knockdown of α-Syn promotes the proliferation of Chrm2 and Chrnb2 cells at the injury site

The proliferation of Chrm2- and Chrnb2-positive cells in the spinal cord injury site of rats was evaluated by 5-bromodeoxyuridine (BrdU) labeling to examine whether knockdown of α-Syn was induced by chrm2 and chrnb2 cells. GFP was transduced with a lentiviral vector expressing the green fluorescence protein, the SCI group was transduced with a blank vector, the LV_SCI group was transduced with a lentiviral vector expressing the target gene SNCA-shRNA, and GFP expression indicates knockout of α-Syn at this site. As shown in Fig.7A-B, the number of Chrm2+BrdU+ and Chrnb2+BrdU+ cells in the SGZ cluster was

significantly increased in LV_SCI rats compared to SCI rats. This result indicated that the new Chrm2 and Chrnb2 cells proliferated in the LV_SCI group and further confirmed the expression of Chrm2 and Chrnb2(Fig.7C-D).

Effect of α-Syn knockdown on SCI neurogenesis and Chrm2 and Chrnb2 subcellular localization

To further investigate the mechanism of action of the cholinergic pathway in spinal cord injury, we determined the expression of Chrm2 and Chrnb2 in neurogenesis and their subcellular localization. DCX (double cortisol) antibodies can be used to specifically label new neurons[11]. We performed multiple immunofluorescence staining on Chrm2, Chrnb2, DCX and GPF in the spinal cord injury sites of the SCI group and LV_SCI group. In Fig.8A-B, we observed that the number of DCX+ Chrm2+ and DCX+ Chrnb2+ double-positive cells in the LV_SCI group was significantly higher than that in the SCI group (Fig.8C-D). GFP was expressed in the cytoplasm, and SNCA was present in the cytoplasm; DCX staining was expressed as filamentous protein, cytoplasmic expression marked the neurite state. Both Chrm2 and Chrnb2 proteins are expressed in the cell membrane and membrane peripheral-secreted proteins. In the LV_SCI group, Chrm2 protein expression was found to increase at the cell-cell junction. Chrnb2 increases expression on the cell membrane in a sheet form, increasing intercellular communication. From the subcellular localization of Chrm2, Chrnb2, DCX and GPF, the LV_SCI group may activate the cholinergic pathway by promoting Chrm2 and Chrnb2 expression and increase the tight junction between cells to further promote neurogenesis at the injury site.

Discussion

Severe and often irreversible defects in spinal cord injury lead to reduced sensorimotor and autonomic function. The secondary injury process of SCI will worsen the neurological outcome, regardless of whether it is organic or functional; therefore, treating this stage should be an important goal of therapy[12]. α-Synuclein is a CNS-enriched protein. An increasing number of studies have reported that α-Syn affects the neurological prognosis in secondary nerve injury. Intervention by various means prevents the death of neurons and promotes functional recovery. In the past several years, there has been evidence that misfolded α-Syn, the major component of the Lewy body, accumulates in the brains of patients with Parkinson's disease (PD) and traumatic CNS-related diseases. The misfolded protein spreads in a virus-like manner between neurons[13]. Usually, misfolded α-Syn also better penetrates the blood-brain barrier. It has been suggested that aggregation of α-Syn is preferentially formed in projection neurons with long, thin, unmyelinated axons[14]. The structural basis for the α-synuclein aggregation of autonomic hyperbranched unmyelinated axons. It is expected that energy/metabolic burden and oxidative stress can be significantly enhanced in these types of neurons, thereby aggravating secondary injury responses[14]. The aggregation of autonomic nerve cells induced by aggregation of α-Syn significantly disturbs the normal neurotransmitter balance, which may be one of the main causes of secondary events.

We used RNA-Seq analysis as an unbiased method[15] to screen for differentially expressed genes in spinal cord injury tissues from surgically modified and knockdown rats in the α-Syn group 28 days after surgery. A total of 191 differentially expressed genes, including 89 upregulated genes and 102 downregulated genes, were screened. Through GO enrichment, it was found that after knocking down α-Syn, the "extracellular matrix", "ion channel activity", and "passive transmembrane transporter activity". KEGG enrichment screened two pathways that are distinctly different and closely related to pathophysiological processes, namely, the cholinergic synapse pathway and the neuroactive ligand-receptor interaction. The 13 differentially expressed genes in the pathway screened two closely related genes, Chrm2 and Chrnb2. RT-qPCR verification, cell proliferation and functional verification revealed that Chrm2 and Chrnb2 play an important role in neurogenesis.

Cholinergic dysfunction has been a familiar topic for many years to researchers of spinal cord injury[16]. Traumatic spinal cord injury (SCI) causes severe disruption of the neuronal circuit, leading to motor function defects. Recovery after spinal cord injury requires regeneration of the disrupted circuit back to its original target. Studies have shown that AAV-NT3 gene therapy combined with exercise can reduce muscle spasm after spinal cord injury by altering the excitability of spinal neurons and motor neurons. In addition, in traumatic CNS injury, another major role of the cholinergic pathway is the "cholinergic anti-inflammatory reflex pathway." Delayed secondary SCI may be caused by a variety of injuries, including oxidative stress, mitochondrial dysfunction, disruption of the blood-spinal barrier, glutamate release disorders, pro-inflammatory cytokines, and other mediators. Studies have found that vagus nerve stimulation (VNS) causes a significant decrease in the systemic inflammatory response by endotoxin in experimental animals[17-18]. This effect is mediated by acetylcholine (ACh), which stimulates nicotinic receptors on spleen macrophages. Therefore, this circuit is called a "cholinergic anti-inflammatory pathway." Inhibition of peripheral macrophages and spinal microglia activation by nicotinic acetylcholine receptor agonists reduces neuropathic pain[19-20].

Excessive activation of microglia after SCI overproduces inflammatory cytokines. The immune and nervous systems are tightly bound, and each system can affect another system in response to an *in vivo* balanced infection or inflammatory disturbance. Both microglia and astrocytes express cholinergic receptors; therefore, it is possible to produce some cholinergic effects through these non-neuronal cells[21]. Activation of cholinergic receptors reduces the release of tumor necrosis factor alpha (TNF-alpha), interleukin 1 beta (IL-1 beta) and interleukin-6 (IL-6) [21]. It is possible that ACh released from immune cells or cholinergic neurons regulates immune function by acting on its receptor in an autocrine/paracrine manner[22-23]. Knocking out α-Syn promotes proliferation of cholinergic neuron receptor cells, thereby promoting the "cholinergic anti-inflammatory pathway" to regulate neuroinflammation and reduce secondary reactions of spinal cord injury. At the same time, Jiang et al. [24]found that the use of nicotine inhibits the infiltration of CCR2 + Ly6C high proinflammatory

monocytes and neutrophils into the CNS by activating nicotinic AChRs in a mouse model, and the reduced proinflammatory cytokines may be a decrease in the number of M1 macrophages regulated by the cholinergic anti-inflammatory pathway. [24]

Muscarinic receptor

The muscarinic acetylcholine receptor (mAChR) is a G-protein coupled receptor that plays an important role in neurogenesis, the survival of newborn neurons, and long-term potentiation. These receptors are divided into five subtypes (M1-M5). M1, M3 and M5 subtypes mediate excitatory functions, while M2 and M4 subtypes mediate inhibitory functions. Interestingly, M2 is an autoreceptor that is found at presynaptic cells and inhibits ACh release. By activating the receptor, the ACh signal is regulated by presynaptic feedback inhibition[25]. Studies have reported that knocking out M1 and M2 receptors promotes increased release of neutrophils and pro-inflammatory cytokines, suggesting that M1 and M2 receptor subtypes have anti-inflammatory effects in inflammation[26].

Nicotinic receptor

Activation of the nicotinic ACh receptor (nAChR) by binding to an agonist results in the influx of Na+ and Ca2+. The degree of permeability of Ca2+ depends on the subunit composition of nAChR because the α7 subunit containing nAChRs has considerably higher Ca2 permeability than the receptor containing the α3 or α4 subunit. This regulation of intracellular Ca2+ levels makes it an important mediator of learning and memory, and it relies on signal transduction involving extracellular signal-regulated kinase 1/2 (ERK 1/2) and cAMP response element binding protein (CREB)[27]. Recently, Mufson EJ et al.[28] reported a decrease in the cholinergic neurotransmitter-related transcript CHRNB2 of neurons in traumatic encephalopathy, which encodes the acetylcholine receptor subunit β2. These findings are consistent with clinical pathology studies demonstrating cholinergic-related defects in human TBI, including reduced ChAT activity and immunoreactivity, as well as downregulation of vAChT and AChE[29]. Although CHRNB2 has not previously been associated with TBI, studies have shown that CHRNB2 may be a candidate gene for neurodegenerative diseases and neuropsychiatric diseases, including schizophrenia[30] and AD[31].

Through GO analysis, the differential gene was mainly enriched in "extracellular matrix", "ion channel activity", and "passive transmembrane transporter activity". The subcellular localization of this study found that Chrm2 and Chrnb2 are mainly expressed in cell membranes and cell-cell junctions. Knockdown of α-Syn significantly increased the expression of Chrm2 and Chrnb2, enhanced cell tight association and transmembrane transport of substances, and enhanced the transmission of intercellular neurotransmitters. This study observed that knockdown of α-Syn after spinal cord injury promoted the recovery of neurological function in rats, possibly due to the reprogramming of the association between

the nerves at the injury site by Chrm2 and Chrnb2. This study clarified that knockdown of α-Syn after SCI promotes the activation of cholinergic nerve and neuroreceptor ligation activity and screens out Chrm2 and Chrnb2 genes, confirms their expression and cell localization, and may further clarify the bile after spinal cord injury in the future. The alkali energy pathway mechanism provides a basis for these properties. In addition, Chrm2 and Chrnb2 subcellular localization are membrane proteins, which are more likely to become drugs and therapeutic targets, providing a structural basis for future clinical transformation[32].

However, the role of the cholinergic system and its related immunoregulation is too broad, and the mechanism governing this phenomenon is complex. This study only initially found the relationship between the α-Syn, SCI and cholinergic pathways, and the specific in-depth mechanism warrants further study.

Knockdown of α-synuclein after spinal cord injury may enhance motor function and promote neurogenesis through enhanced cholinergic signaling pathways and neuroreceptor interactions. This study not only further clarifies the understanding of the mechanism of knockdown of α-synuclein on SCI but also helps to guide the treatment strategy for SCI.

Conclusions

Knockdown of α-synuclein after spinal cord injury enhance motor function and promote neurogenesis probably through enhancing cholinergic signaling pathways and neuroreceptor interactions. This study not only further clarifies the understanding of the mechanism of knockdown of α-synuclein on SCI but also helps to guide the treatment strategy for SCI.

Abbreviations

SCI：Spinal Cord Injury；α-Syn：α-Synuclein；BBB：Basso, Beatlie, Bresnahan；RT-qPCR：Real-time Quantitative Polymerase Chain Reaction；RNA-seq：RNA Sequencing；BrdU：Bromodeoxyuridine；shRNA：Short hairpin RNA；LV：Lentivirus；CNS：Central Nervous System；mAChR：Muscarinic Acetylcholine Receptor；nAChR：Nicotinic Acetylcholine Receptor；Chrm2：Muscarinic M2 Cholinergic Receptor；Chrnb2：Cholinergic Receptor Nicotinic Beta 2 Subunit. VNS：Vagus Nerve Stimulation.

Declarations

Acknowledgements

We are grateful for the technical support provided by Peking University Third Hospital Central Laboratory. We also thank to the Bioinformatics Technology Service provided by Biotech Information Platform of Major Biotechnology Co., Ltd of China.

Funding

This work was funded by the National Natural Science Foundation of China (grant number 11472018 to MW. Zhou, the corresponding author) .We also thank the Young Scientist fund of the National Natural Science Foundation of China (grant number 1150020073 to N.Liu) for financial support.

Availability of data and materials

RNA-Seq raw data have been deposited in the NCBI Sequence Read Archive (SRA, https://submit.ncbi.nlm.nih.gov/subs/sra/SUB5917896/overview).Supporting code is available as follows.Accession IDs for *Rattus norvegicus* BioProject = PRJNA552942 BioSample = SAMN12222084 - SAMN12222092 (9 objects) SRA = SRR9448449 - SRR9448455 9 objects.

Authors' contributions

M.W.Z., H.Z.and B.F.Y. conceived and designed the study, M.W.Z.coordinated the project and partly wrote the manuscript. H.Z.and B.F.Y. performed animals management and bio-samples collection. H.Z., B.F.Y., N.L., Y.Y.Y., H.Y.X. designed analyses, performed bioinformatic analyses and partly wrote the manuscript. H.Z., B.F.Y.and X.X.L. performed validation experiments. M.W.Z. supervised and performed bioinformatic analyses. H.Z. and B.F.Y. wrote, revised, and revised the article. All these authors read and approved the final manuscript.

Authors information

Affiliations

Department of Rehabilitation Medicine, Peking University Third Hospital, 49 North Garden Road, Beijing 100191, China

Hong Zeng, Nan Liu, Yan-yan Yang , Hua-yi Xing , Xiao-xie Liu , Mou-wang Zhou

Department of Hand Surgery, Huashan Hospital, Fudan University, Shanghai 200040, China

Bao-fu Yu

Corresponding author

Correspondence to Mou-wang Zhou

Ethics declarations

Ethics approval and consent to participate

All experimental procedures were carried out in accordance with the Chinese Guidelines of Animal Care and Welfare, and the study was approved by the Animal Welfare Ethics Branch of the Peking University Bioethics Committee.

Consent for publication

Not applicable.

Competing Interest

The authors declare that they have no competing interests.

Publisher's Note

Springer Nature remains neutral with regard to jurisdictional claims in published maps and institutional affiliations.

References

1. Duan H, Ge W, Zhang A, Xi Y, Chen Z, Luo D, *et al*: Transcriptome analyses reveal molecular mechanisms underlying functional recovery after spinal cord injury. *Proc Natl Acad Sci U S A*. 2015,112(43).

2. Alizadeh A, Dyck SM, Kataria H, Shahriary GM, Nguyen DH, Santhosh KT, Karimi-Abdolrezaee S: Neuregulin-1 positively modulates glial response and improves neurological recovery following traumatic spinal cord injury. *Glia* 2017, 65(7):1152-1175.

3. Liu S, Chen Z: Employing Endogenous NSCs to Promote Recovery of Spinal Cord Injury. *Stem Cells Int* 2019, 2019:1958631.

4. Rosich K, Hanna BF, Ibrahim RK, Hellenbrand DJ, Hanna A: The Effects of Glial Cell Line-Derived Neurotrophic Factor after Spinal Cord Injury. *J Neurotrauma* 2017, 34(24):3311-3325.

5. Amanat M, Vaccaro AR: Reducing alpha-synuclein in spinal cord injury: A new strategy of treatment. *J Neurosci Res* 2019, 97(7):729-732.

6. Goedert M: Alzheimer's and Parkinson's diseases: The prion concept in relation to assembled Abeta, tau, and alpha-synuclein. *Science* 2015, 349(6248):1255555.

7. Rocha EM, De Miranda B, Sanders LH: Alpha-synuclein: Pathology, mitochondrial dysfunction and neuroinflammation in Parkinson's disease. *Neurobiol Dis* 2018, 109(Pt B):249-257.

8. Feng GY, Liu J, Wang YC, Wang ZY, Hu Y, Xia QJ, Xu Y, Shang FF, Chen MR, Wang F *et al*: Effects of Alpha-Synuclein on Primary Spinal Cord Neurons Associated with Apoptosis and CNTF Expression. *Cell Mol Neurobiol* 2017, 37(5):817-829.

9. Wang H, Yu Q, Ding X, Hu X, Hou K, Liu X, Nie S, Xie M: RNA-seq based elucidation of mechanism underlying Ganoderma atrum polysaccharide induced immune activation of murine myeloid-derived dendritic cells. *Journal of Functional Foods* 2019, 55:104-116.

10. Ma Q, Chen C, Zeng Z, Zou Z, Li H, Zhou Q, Chen X, Sun K, Li X: Transcriptomic analysis between self- and cross-pollinated pistils of tea plants (Camellia sinensis). *BMC Genomics* 2018, 19(1):289.

11. Balta EA, Wittmann MT, Jung M, Sock E, Haeberle BM, Heim B, von Zweydorf F, Heppt J, von Wittgenstein J, Gloeckner CJ *et al*: Phosphorylation Modulates the Subcellular Localization of SOX11. *Front Mol Neurosci* 2018, 11:211.

12. Flores-Cuadrado A, Saiz-Sanchez D, Mohedano-Moriano A, Martinez-Marcos A, Ubeda-Banon I: Neurodegeneration and contralateral alpha-synuclein induction after intracerebral alpha-synuclein injections in the anterior olfactory nucleus of a Parkinson's disease A53T mouse model. *Acta Neuropathol Commun* 2019, 7(1):56.

13. Braak H, Del Tredici K: Neuroanatomy and pathology of sporadic Parkinson's disease. *Adv Anat Embryol Cell Biol*. 2009, 201:1-119.

14. Uchihara T, Giasson BI: Propagation of alpha-synuclein pathology: hypotheses, discoveries, and yet unresolved questions from experimental and human brain studies. *Acta Neuropathol* 2016, 131(1):49-73.

15. Xiang X, Yu Y, Tang X, Chen M, Zheng Y, Zhu S: Transcriptome Profile in Hippocampus During Acute Inflammatory Response to Surgery: Toward Early Stage of PND. *Front Immunol* 2019, 10:149.

16. Anglister L, Cherniak M, Lev-Tov A: Ascending pathways that mediate cholinergic modulation of lumbar motor activity. *J Neurochem* 2017, 142 Suppl 2:82-89.

17. Li DJ, Fu H, Tong J, Li YH, Qu LF, Wang P, Shen FM: Cholinergic anti-inflammatory pathway inhibits neointimal hyperplasia by suppressing inflammation and oxidative stress. *Redox Biol* 2018, 15:22-33.

18. Di Cesare Mannelli L, Zanardelli M, Ghelardini C: Nicotine is a pain reliever in trauma- and chemotherapy-induced neuropathy models. *Eur J Pharmacol* 2013, 711(1-3):87-94.

19. Hoover DB: Cholinergic modulation of the immune system presents new approaches for treating inflammation. *Pharmacol Ther* 2017, 179:1-16.

20. Kiguchi N, Kobayashi D, Saika F, Matsuzaki S, Kishioka S: Inhibition of peripheral macrophages by nicotinic acetylcholine receptor agonists suppresses spinal microglial activation and neuropathic pain in mice with peripheral nerve injury. *J Neuroinflammation* 2018, 15(1):96.

21. Maurer SV, Williams CL: The Cholinergic System Modulates Memory and Hippocampal Plasticity via Its Interactions with Non-Neuronal Cells. *Front Immunol* 2017, 8:1489.

21. Maurer SV, Williams CL: The Cholinergic System Modulates Memory and Hippocampal Plasticity via Its Interactions with Non-Neuronal Cells. *Front Immunol* 2017, 8:1489.

22. Liu Z, Wang L, Lv Z, Zhou Z, Wang W, Li M, Yi Q, Qiu L, Song L: The Cholinergic and Adrenergic Autocrine Signaling Pathway Mediates Immunomodulation in Oyster Crassostrea gigas. *Front Immunol* 2018, 9:284.

23. Sui G, Fry CH, Montgomery B, Roberts M, Wu R, Wu C: Purinergic and muscarinic modulation of ATP release from the urothelium and its paracrine actions. *Am J Physiol Renal Physiol* 2014, 306(3):F286-298.

24. Jiang W, St-Pierre S, Roy P, Morley BJ, Hao J, Simard AR: Infiltration of CCR2+Ly6Chigh Proinflammatory Monocytes and Neutrophils into the Central Nervous System Is Modulated by Nicotinic Acetylcholine Receptors in a Model of Multiple Sclerosis. *J Immunol* 2016, 196(5):2095-2108.

24. Jiang W, St-Pierre S, Roy P, Morley BJ, Hao J, Simard AR: Infiltration of CCR2+Ly6Chigh Proinflammatory Monocytes and Neutrophils into the Central Nervous System Is Modulated by Nicotinic Acetylcholine Receptors in a Model of Multiple Sclerosis. *J Immunol* 2016, 196(5):2095-2108.

25. Shin SS, Dixon CE: Alterations in Cholinergic Pathways and Therapeutic Strategies Targeting Cholinergic System after Traumatic Brain Injury. *J Neurotrauma* 2015, 32(19):1429-1440.

26. Kistemaker LE, Bos IS, Hylkema MN, Nawijn MC, Hiemstra PS, Wess J, Meurs H, Kerstjens HA, Gosens R: Muscarinic receptor subtype-specific effects on cigarette smoke-induced inflammation in mice. *Eur Respir J* 2013, 42(6):1677-1688.

27. Thomas GM, Huganir RL: MAPK cascade signalling and synaptic plasticity. *Nat Rev Neurosci* 2004, 5(3):173-183.

28. Mufson EJ, He B, Ginsberg SD, Carper BA, Bieler GS, Crawford F, Alvarez VE, Huber BR, Stein TD, McKee AC *et al*: Gene Profiling of Nucleus Basalis Tau Containing Neurons in Chronic Traumatic Encephalopathy: A Chronic Effects of Neurotrauma Consortium Study. *J Neurotrauma* 2018, 35(11):1260-1271.

29. Pike BR, Hamm RJ: Activating the posttraumatic cholinergic system for the treatment of cognitive impairment following traumatic brain injury.*Pharmacol Biochem Behav.* 1997,57(4):785-91.

30. De Luca V, Voineskos S, Wong G, Kennedy JL: Genetic interaction between alpha4 and beta2 subunits of high affinity nicotinic receptor: analysis in schizophrenia. *Exp Brain Res* 2006, 174(2):292-296.

31. Cook LJ, Ho LW, Taylor AE, Brayne C, Evans JG, Xuereb J, Cairns NJ, Pritchard A, Lemmon H, Mann D *et al*: Candidate gene association studies of the alpha 4 (CHRNA4) and beta 2 (CHRNB2) neuronal

nicotinic acetylcholine receptor subunit genes in Alzheimer's disease. *Neurosci Lett* 2004, 358(2):142-146.

32. Mingarro I, von Heijne G, Whitley P: Membrane-protein engineering.Trends Biotechnol. 1997,15(10):432-7.

33. Squair JW, Ruiz I, Phillips AA, Zheng MMZ, Sarafis ZK, Sachdeva R, Gopaul R, Liu J, Tetzlaff W, West CR *et al*: Minocycline Reduces the Severity of Autonomic Dysreflexia after Experimental Spinal Cord Injury. *J Neurotrauma* 2018, 35(24):2861-2871.

34. Basso DM, Beattie MS, Bresnahan JC: A sensitive and reliable locomotor rating scale for open field testing in rats. *J Neurotrauma.* 1995,12:1-21.

35. Li B, Dewey CN: RSEM: accurate transcript quantification from RNA-Seq data with or without a reference genome. *BMC Bioinformatics* 2011;12:323.

36. Robinson MD, McCarthy DJ, Smyth GK: edgeR: a Bioconductor package for differential expression analysis of digital gene expression data. *Bioinformatics* 2010;26:139-40.

37. Xie C, Mao X, Huang J, Ding Y, Wu J, Dong S, *et al*: KOBAS 2.0: a web server for annotation and identification of enriched pathways and diseases. *Nucleic Acids Res* 2011;39:W316-22.

37. Xie C, Mao X, Huang J, Ding Y, Wu J, Dong S, *et al*: KOBAS 2.0: a web server for annotation and identification of enriched pathways and diseases. *Nucleic Acids Res* 2011;39:W316-22.

38. Sahinkaya FR, Milich LM, McTigue DM: Changes in NG2 cells and oligodendrocytes in a new model of intraspinal hemorrhage. *Exp Neurol* 2014, 255:113-126.

Figures

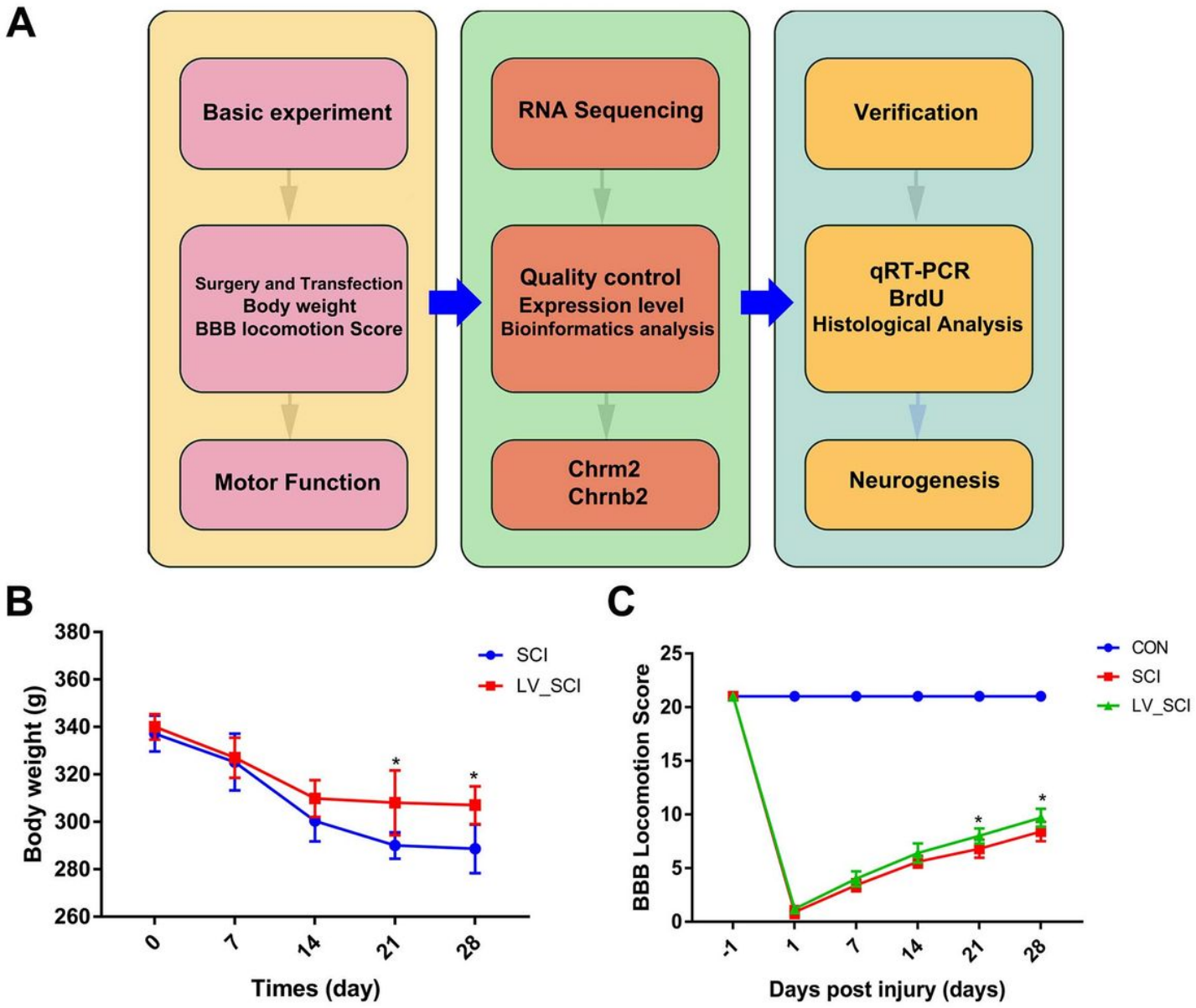

Figure 1

The motor behavior is improved with knockdown α-Syn treatment. (A) Timeline of experimental protocol. (B) Changes in body weight of rats. n = 5. (C) Quantification of the BBB Scale score on day 28 of each group. n = 5. * P< 0.05.

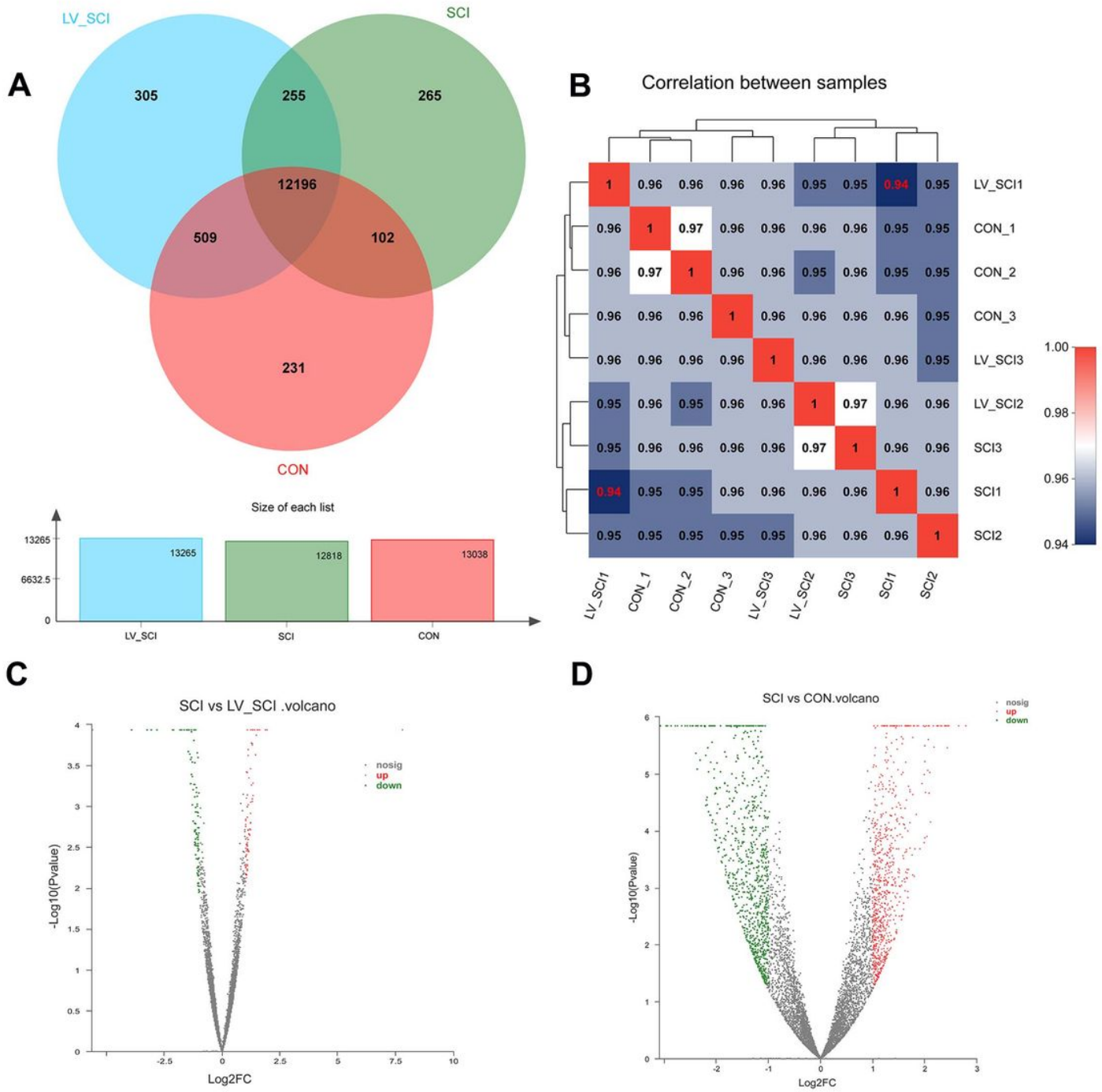

Figure 2

Changes in mRNA expression profiles between groups. (A) The amount of expression of the three groups in the entire transcriptome. (B) Heat map of mRNA transcripts showing correlations between samples. (C) Volcano plots show up- and down-regulated mRNA transcripts in the LV_SCI vs SCI group. (D) Volcano plots indicate up- and down-regulated mRNA transcripts in the CON vs SCI group.

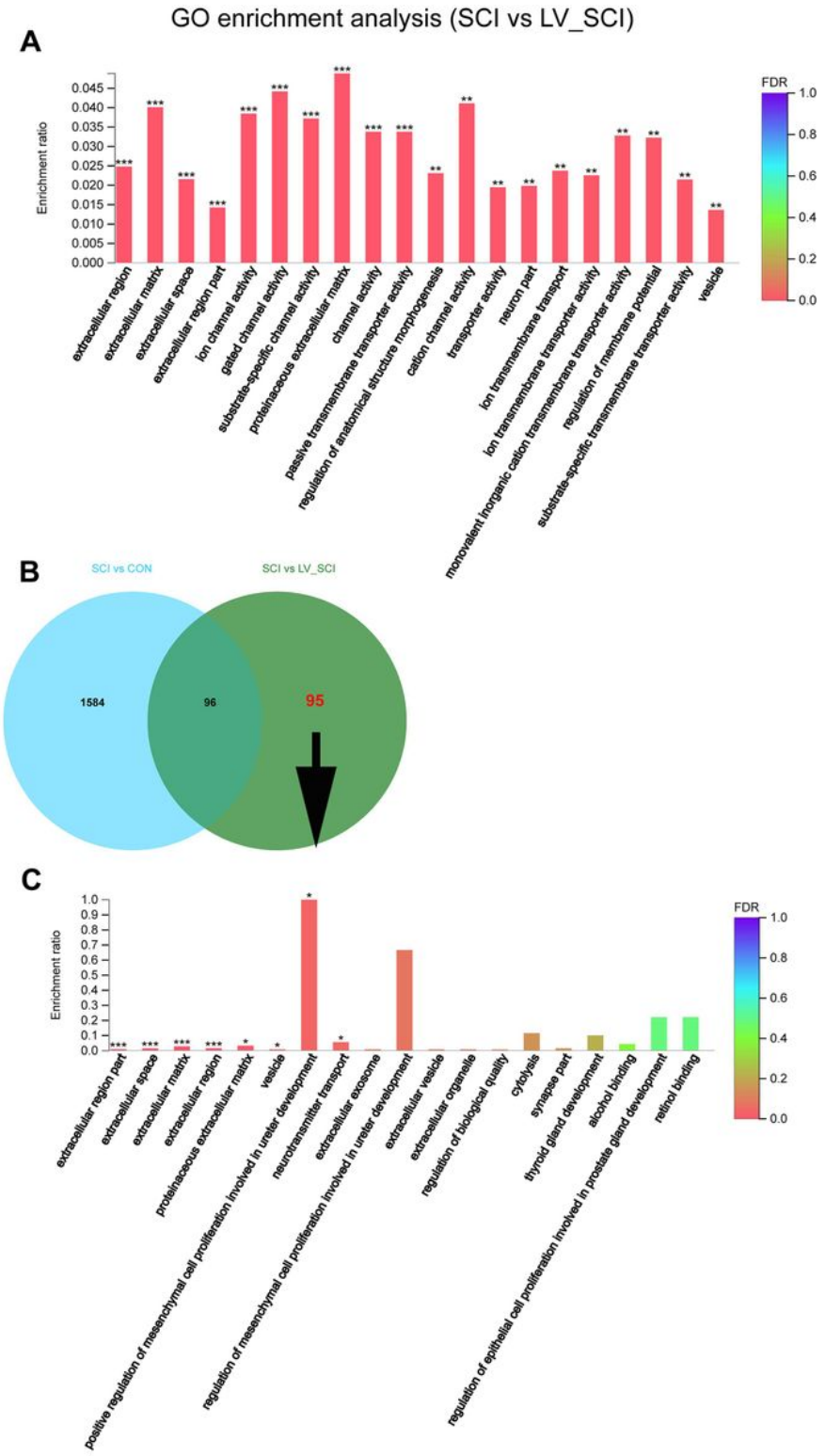

Figure 3

GO Enrichment Analysis of DEGs. (A) GO enrichment histogram of SCI and LV_SCI group DEGs. (B) Venn diagram between the three groups. (C) Compared to SCI, CON group, LV_SCI group has an exclusive GO enrichment histogram of DEGs.

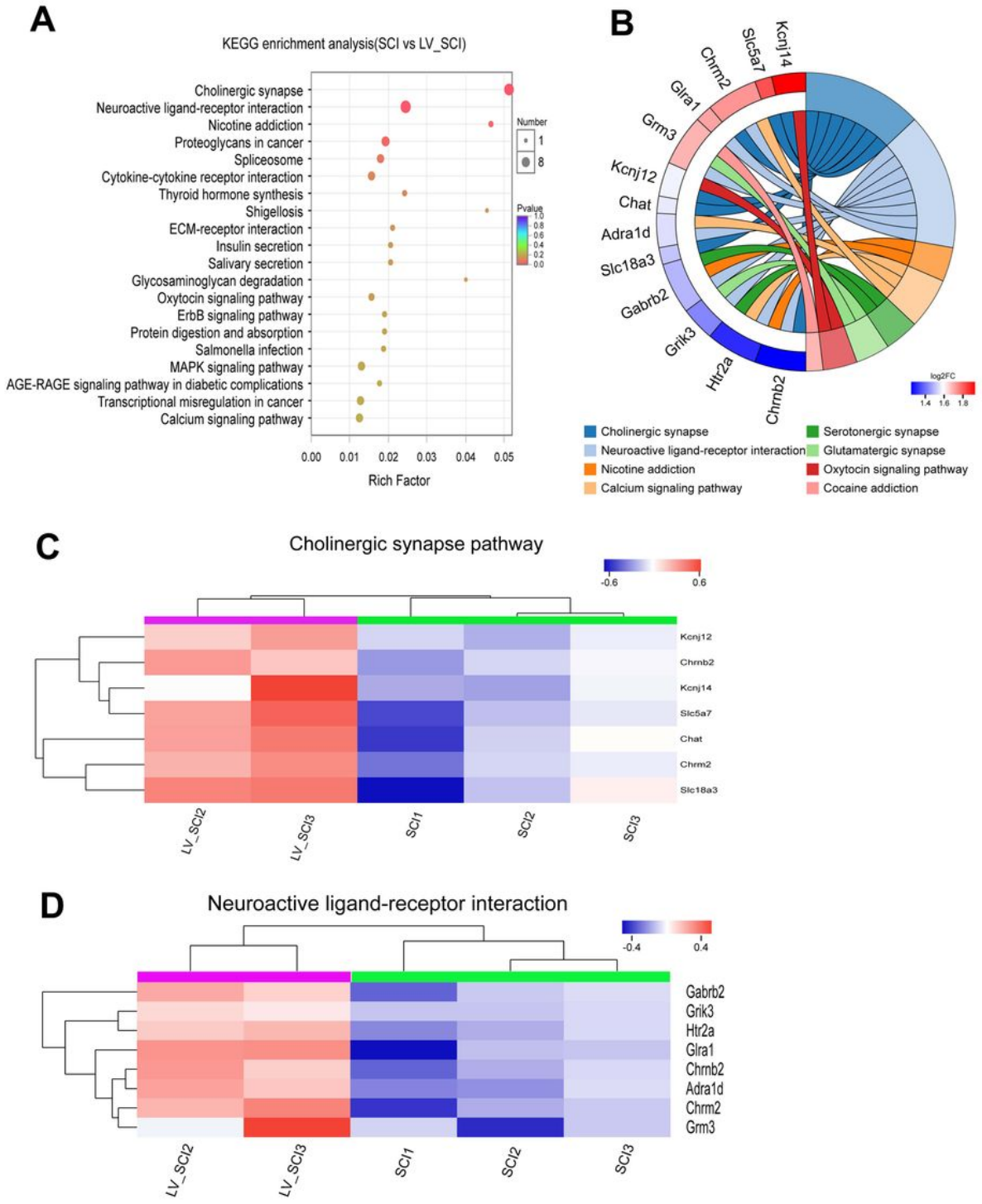

Figure 4

The DEGs with KEGG pathway enrichment occurred in 2 pathways. (A) KEGG pathway enrichment analysis of DEGs. (B) The KEGG pathway of DEGs enriches the chord diagram. (C-D) Heat maps of DEGs of cholinergic signaling pathways and neuroreceptor interactions pathways.

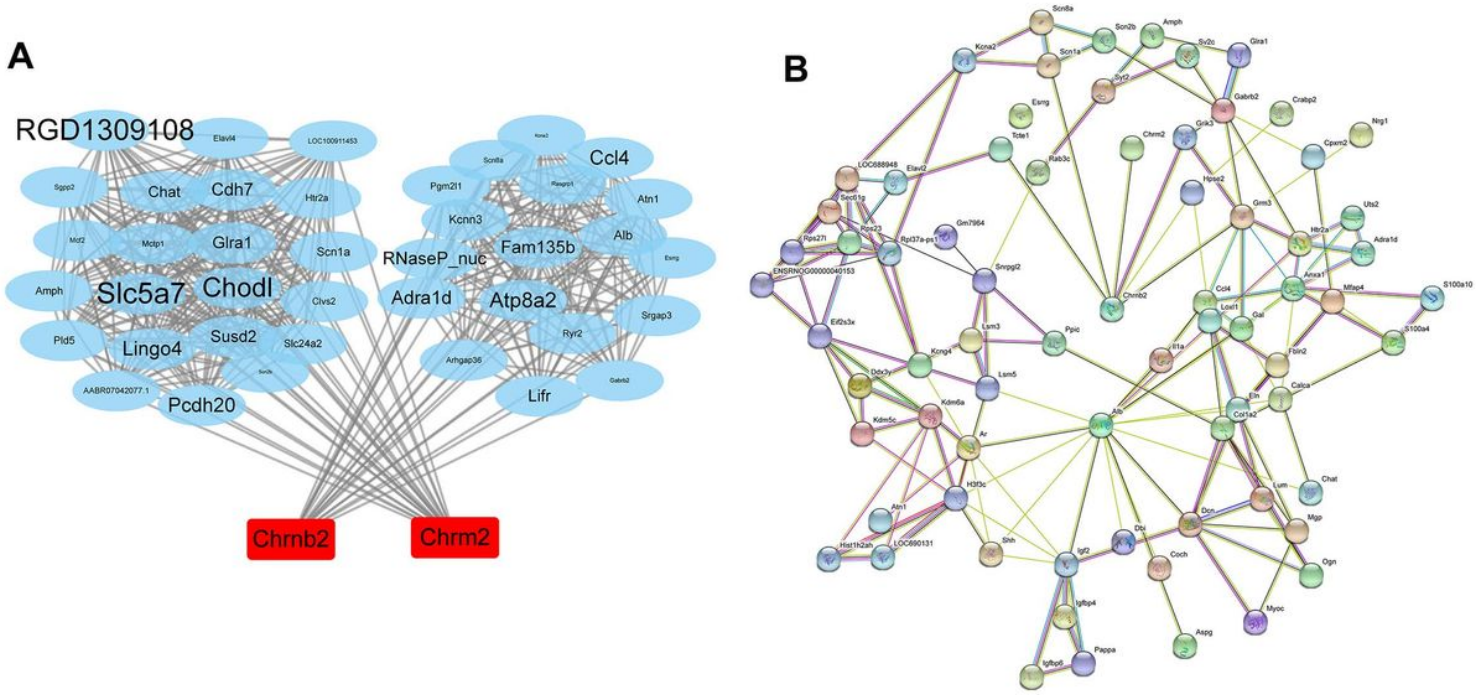

Figure 5

Differential genes and proteins interaction network analysis. (A) Interplay analysis of expression-related genes with Chrm2 and Chrnb2 as genes of interest. (B) Protein interaction of DEGs between SCI and LV_SCI group.

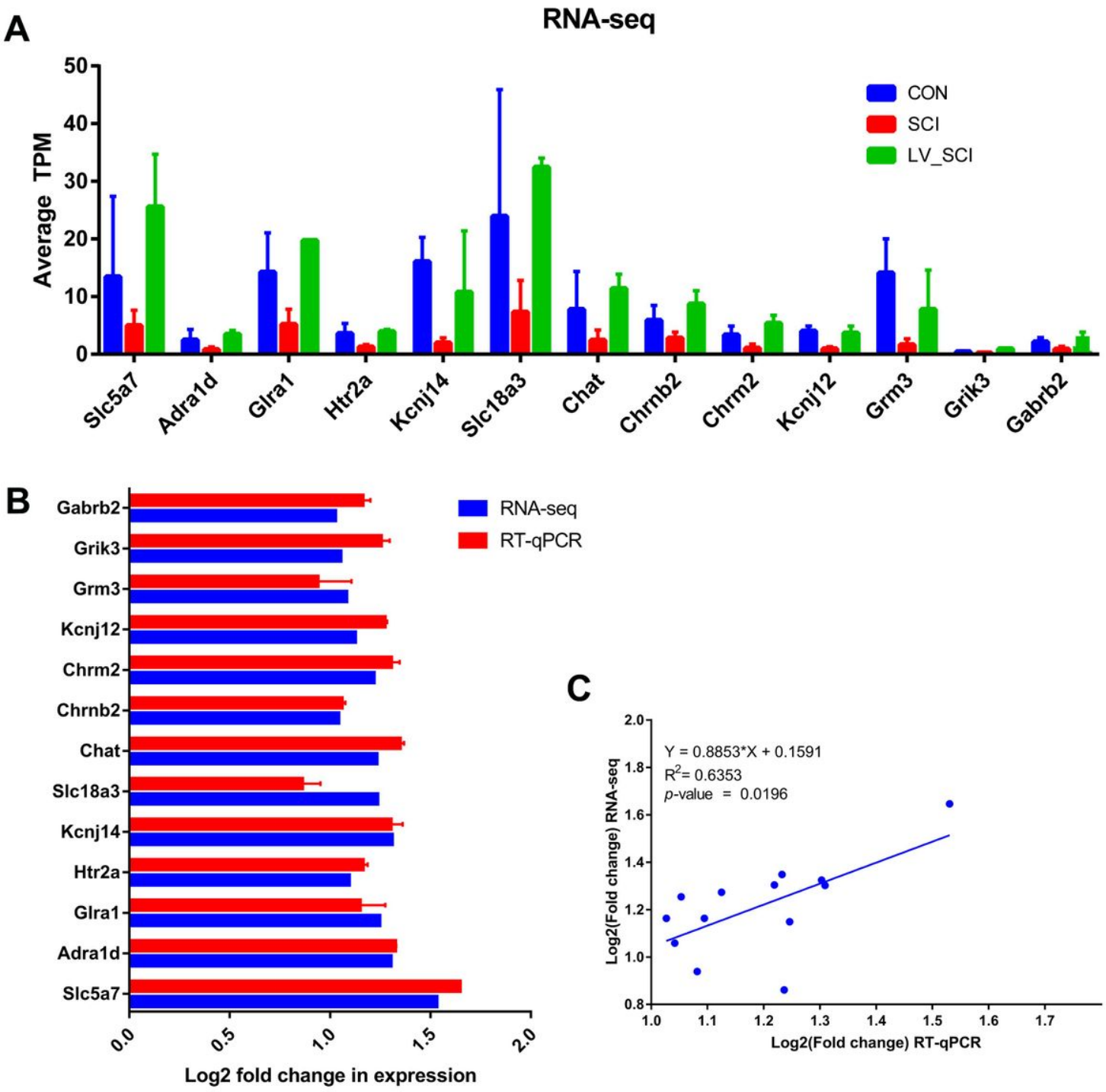

Figure 6

RT-qPCR validation of RNA-seq. (A) Average TPM values of 13 DEGs obtained in RNA-seq. (B) Comparison of transcript expression in terms of fold change was measured by RNA-Seq and qPCR. (C) Correlation analysis of RT-qPCR and RNA-seq.

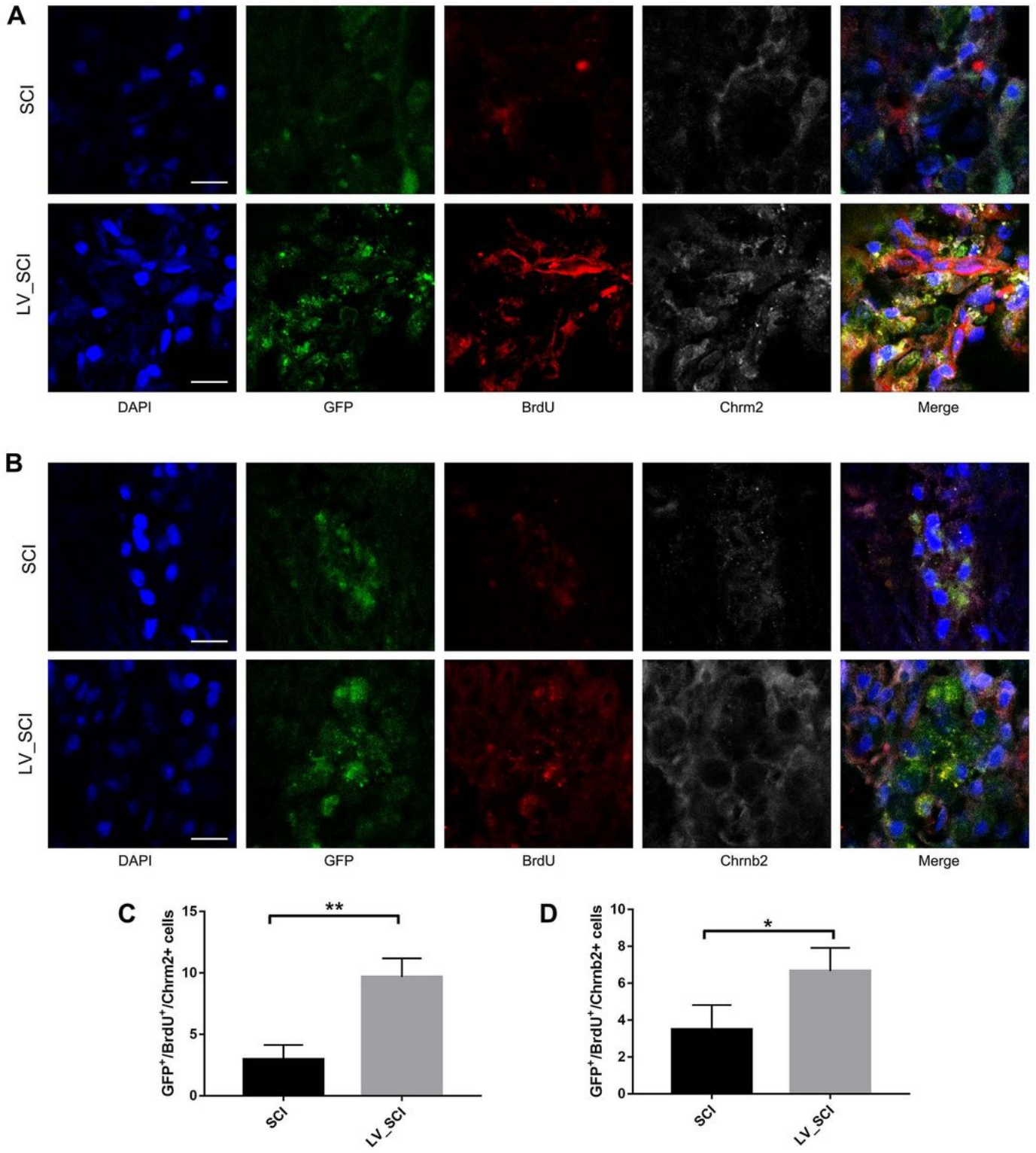

Figure 7

Histological analysis of Chrm2 and Chrnb2 cells proliferation at the injury site. (A) Representative images showing GFP+/BrdU+/Chrm2+ triple staining by immunofluorescence. Scale bar = 35 μm. (B) Representative images showing GFP+/BrdU+/Chrnb2+ triple staining by immunofluorescence. Scale bar = 35 μm. (C-D) Quantitative analysis results from Figure A, B. n = 3. *=p <0.05.

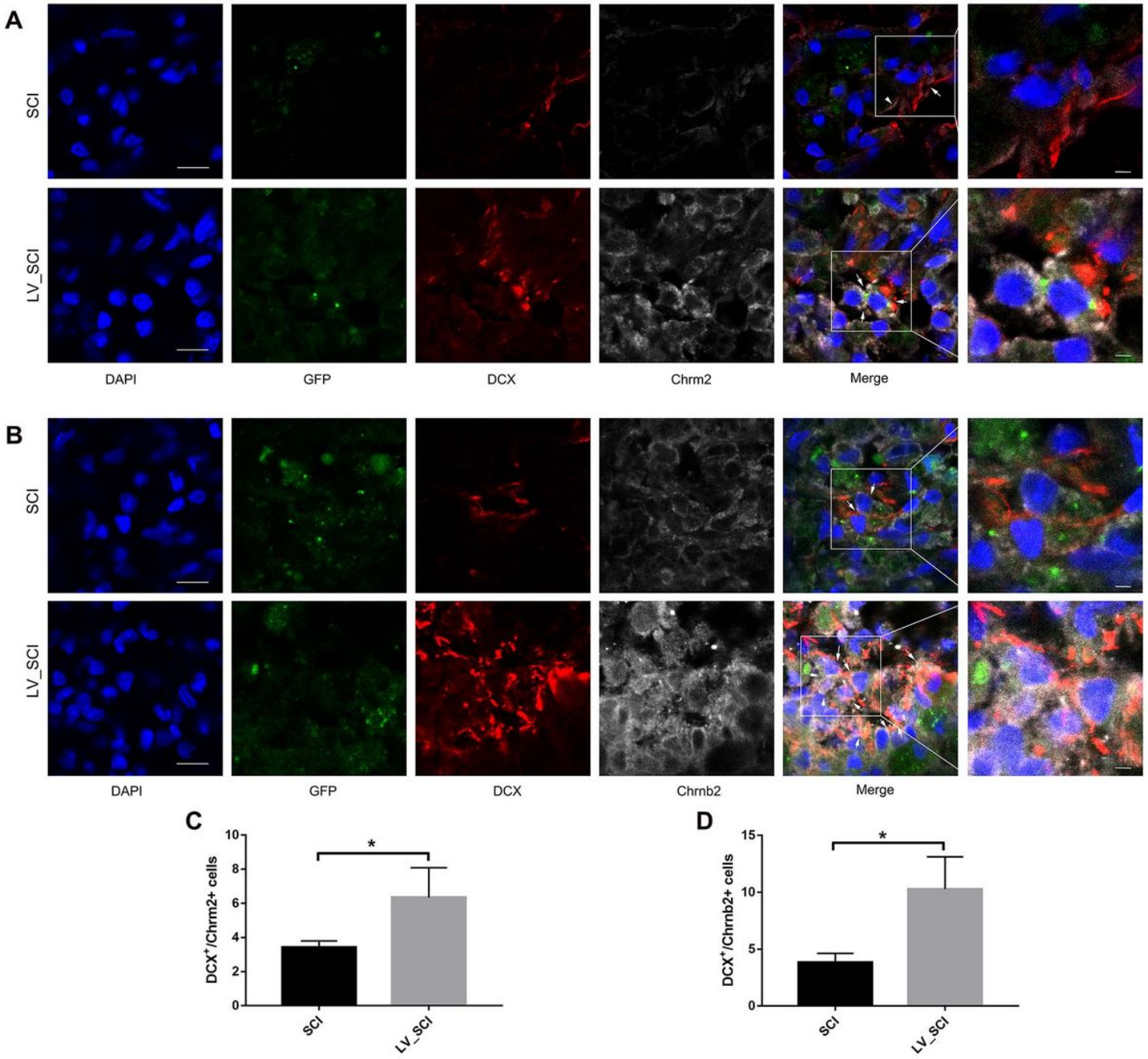

Figure 8

Facilitated the neurogenesis and Chrm2 and Chrnb2 subcellular localized at the injury site after spinal cord injury. (A) Representative images showing GFP+/BrdU+/Chrm2+ triple staining by immunofluorescence, Scale bar = 35 μm. (B) Representative images showing GFP+/BrdU+/Chrnb2+ triple staining by immunofluorescence. Scale bar = 35 μm. (C-D) Quantitative analysis results from Figure A, B. n = 3. *=p <0.05.

Supplementary Files

This is a list of supplementary files associated with this preprint. Click to download.

- supplement1.xls
- supplement1.xlsx
- supplement3.xlsx
- supplement4.pdf
- supplement4.xlsx
- supplement6.tif
- supplement6.xls
- supplement8.xlsx
- supplement8.xls
- supplement8.tif
- supplement11.pdf
- supplement12.tif